Sensors and Materials, Vol. 35, No. 10 (2023) 4769–4779
MYU Tokyo

S & M 3429

Enzyme-immobilized Screen-printed Sensor for One Drop of Sample Using Porous Silica Spheres

Shunsuke Fujii,[1,2] Akiko Yoshida,[3,4] Tracy T. Chuong,[2] Yuka Minegishi,[2] Yuta Nishina,[5] Hirotomo Nishihara,[4] Kouji Masumoto,[1*] and Tetsuji Itoh[2**]

[1]Department of Pediatric Surgery, Faculty of Medicine, University of Tsukuba, Tsukuba, Ibaraki 305-8575, Japan
[2]National Institute of Advanced Industrial Science and Technology (AIST), Sendai, Miyagi 983-8551, Japan
[3]R & D Department, Techno Medica Co., Ltd., Yokohama, Kanagawa 224-0041, Japan
[4]Institute of Multidisciplinary Research for Advanced Materials (IMRAM)/Advanced Institute for Materials Research (WPI-AIMR), Tohoku University, Sendai, Miyagi 980-8577, Japan
[5]Graduate School of Natural Science and Technology, Okayama University, Kita-ku, Okayama 700-8530, Japan

(Received April 27, 2023; accepted August 24, 2023)

Keywords: biosensor, enzyme electrode, mediator, screen-printed device, porous silica

A sensor chip that can detect enzyme electrode reactions with a sample volume as small as 20 μL has been developed using screen-printing technology with porous silica spheres (PSSs). PSSs are spherical particles of silica with mesoporous pores, a material with a large specific surface area. Other material properties of PSSs include good dispersibility, high mechanical strength, and the ability to be synthesized with precisely controlled mesopore sizes. These advantages support the increased adsorption of enzymes to create highly sensitive sensors. The electrode was designed as follows: carbon paste (CP) with PSSs was used as the working electrode, glucose dehydrogenase (GDH) was used as the enzyme, and quinoline-5,8-dione (QD) was used as the mediator of electron transfer to induce a glucose dehydrogenation reaction. The sensitivity of the sensor was demonstrated through the detection of glucose. The glucose sensor showed reliable sensitivity between 1 and 60 mM glucose, which is comparable to the detection range of a traditional working electrode such as platinum. Furthermore, the GDH had a minimal reduction in activity over repeated usage. This device demonstrates the ability to create an equally sensitive but less expensive and reusable sensor that has the potential to better suit general applications.

1. Introduction

Recent efforts have been directed toward the development of biosensors that combine biological detection with physical transducers.[1–6] In particular, amperometric biosensors using immobilized enzyme electrodes can provide high sensitivity, high selectivity, and short response time without the need for large or complex equipment. These sensors have been shown to detect glucose or lactate[7–12] at low concentrations reliably and reproducibly. Parallel to biosensor development, active development is also taking place to simplify sensor production, specifically

*Corresponding author: e-mail: kmasu@md.tsukuba.ac.jp
**Corresponding author: e-mail: tetsu-itou@aist.go.jp
https://doi.org/10.18494/SAM4473

ISSN 0914-4935
https://myukk.org/

on the stability and longevity of the sensors as analytical instruments. Stability is mainly dependent on the rate of denaturation or inactivation of the enzyme employed.[13–16] Novel immobilization methods[4,16–18] used to enhance enzyme stability and optimize the surrounding microenvironment through material choice[19–22] have been investigated. One of the best immobilization methods to stabilize enzymes to retain good catalytic activity is to encapsulate the enzyme in mesoporous silica (MPS) materials. MPS materials inherently have high surface areas and pore volumes, tunable pore sizes to accommodate enzymes of different dimensions, and excellent mechanical stability.[23,24] Our previous studies using an enzyme-immobilized electrode in a stirred-batch cell showed that high-performance biosensors can be constructed using immobilized enzymes within MPS materials.[25–31]

However, when this technique is combined with screen-printing, a range of complications occur. At minimum, the particles can be non-uniformly distributed, resulting in the poor reproducibility of the detection quality; at worst, the pores can be clogged, which inhibits the diffusion of the substrates and the electron mediator, resulting in device failure. We explored porous silica spheres (PSSs) with a uniform particle size as candidate materials to resolve this issue. The pore and particle sizes of PSSs can be controlled over a wide range while maintaining a small variance, which allows them to be arranged uniformly on the electrode. The enzyme can then be immobilized on the PSS layer, and stability can be obtained as demonstrated in our previous papers,[25,29] where carbon-coated PSS electrodes were arranged in a very small area.[32]

In this paper, we report on the development of a highly stable, sensitive, and reusable sensor using PSSs as an enzyme immobilization host, fabricated by screen-printing.

2. Materials and Methods

2.1 Materials

Pyrroloquinoline quinone-dependent glucose dehydrogenase (PQQ-GDH) (1040 U/mg) from microorganisms was purchased from Toyobo Co., Ltd. in Japan. PQQ-GDH was dissolved in water at a concentration of 2.8 U/μL. Sodium dihydrogen phosphate (NaH_2PO_4) and disodium hydrogen phosphate (Na_2HPO_4) were obtained from Kanto Chemical Co., Ltd., Japan. Phosphate buffer (50 mM, pH 7) was prepared by mixing NaH_2PO_4 and Na_2HPO_4. Potassium ferricyanide (PF) and quinoline-5,8-dione (QD), a water-soluble quinone mediator, were used as mediators of electron transfer.[32,33] PF was purchased from Sigma-Aldrich, and the synthesis of QD is described below (see Sect. 2.2). PF or QD was dissolved in phosphate buffer to 5 mM, pH 7. D (+)-glucose was obtained from Fujifilm Wako Pure Chemicals Co., Ltd. and dissolved in phosphate buffer to 100 mM, pH 7.

2.2. Synthesis of QD[32,33]

A solution of 5-hydroxyquinoline (312 mg, 2.14 mmol) in acetonitrile (30 mL) was cooled to 0 °C under argon atmosphere. Then, [bis(trifluoroacetoxy)iodo] benzene (PIFA) (2 g, 4.7 mmol)

was dissolved in 2:1 acetonitrile–water solution (60 mL). The PIFA solution was added dropwise to the precooled solution of 5-hydroxyquinoline and the mixture was stirred for 1 h. The reaction mixture was concentrated under reduced pressure, resulting in a dark brown aqueous solution. The aqueous solution was extracted with ethyl acetate (20 mL) three times. The organic extract was washed with brine (50 mL), dried over magnesium sulfate, filtered, and concentrated under reduced pressure to give a dark yellow residue. The residue was purified by silica gel column chromatography eluting with 1:4 ethyl acetate–hexanes to give crystals.

2.3. Fabrication of three-electrode sensor chips

A sensor chip consisting of a three-electrode system was fabricated by screen-printing (Fig. 1). On an aluminum oxide substrate, a working electrode and a counter electrode were placed with sintering platinum (Pt) paste (Tanaka Kikinzoku Kogyo K.K., Japan) and wired with sintering silver paste (Mitsuboshi Belting Ltd., Japan). A Ag/AgCl reference electrode was created by overlaying silver chloride on silver. Thermosetting silver paste was used for the contacts between the silver wiring part and the Pt electrode part. Thermosetting-type epoxy resin paste and polyester resin paste were laminated thereon to define the area of the electrode

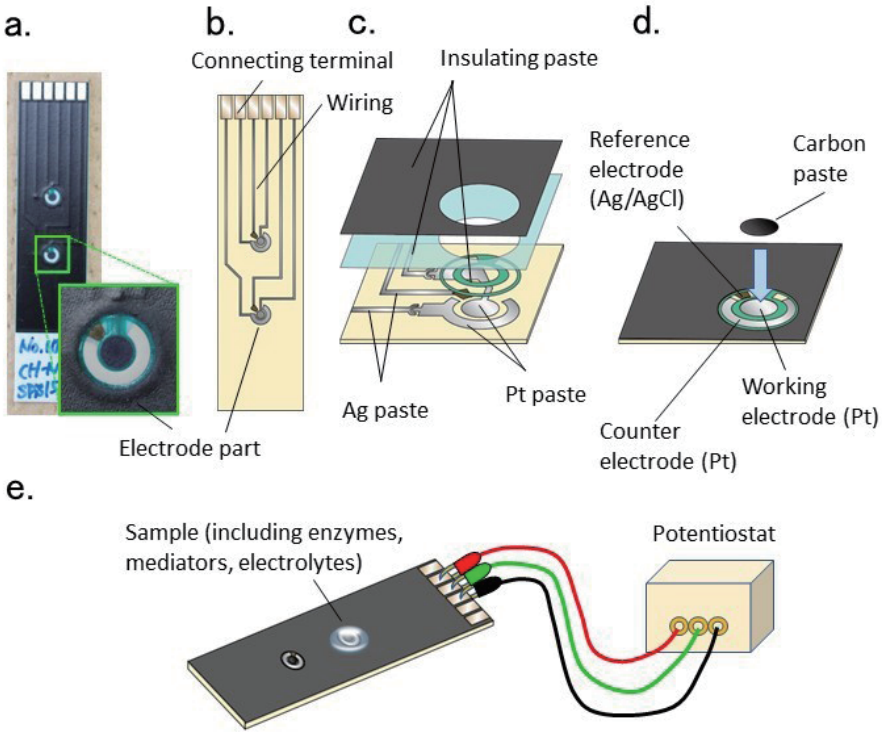

Fig. 1. (Color online) Fabrication of electrode sensor chip. (a) Actual photo of sensor chip (sensor chip size: 5 × 1 cm^2, working electrode: ϕ 1 mm). (b) Wiring diagram of sensor chip. (c) Structure of sensor chip laminated by screen-printing. (d) A CP electrode was fabricated by the screen-printing of CP on a platinum working electrode. (e) Electrochemical analysis with electrode sensor chip. Electrochemical analysis was performed by connecting the connecting terminal of the sensor chip to a potentiostat and dropping 20 μL of sample (including enzymes, mediator, and electrolyte) onto the electrode.

section and to protect the wiring section. Carbon paste (CP) working electrodes were prepared by screen-printing CH-N carbon ink (Jujo Chemical Co., Ltd., Japan) onto the Pt working electrode.

2.4. Electrochemical analysis

For electrochemical analysis, the sensor chip was used in combination with a potentiostat HX-5000 (Hokuto Denko Corporation, Japan) [Fig. 1(e)]. First, a mixture of 5 μL of PQQ-GDH solution and 5 μL of mediator solution was placed on the working electrode. Then, a mixture of 5 μL of D-glucose and 5 μL of mediator solution was added to induce the following enzymatic reaction:

$$\text{D-glucose} + \text{acceptor} \xrightarrow{\text{GDH}} \text{D-glucono-1,5-lactone} + \text{reduced acceptor}. \quad (1)$$

The final concentrations of PQQ-GDH and the mediator in the mixed solution were 0.7 U/μL and 2.5 mM, respectively. Note that glucose was diluted fourfold from its original concentration in the mixed solution. The sensing performance for the above enzymatic reaction was examined by cyclic voltammetry and amperometry. Cyclic voltammetry was performed for six cycles in a potential window of −0.5 to 0.8 V, and the redox currents at the third cycle were compared. For amperometry, a constant potential (0.3 V) was applied, and after the background current stabilized for 120 s, the D-glucose solution was dropped onto the working electrode. Fifty seconds after the D-glucose solution was dropped (t = 170 s), the output currents were compared. A calibration curve was created by plotting the change in output current across a range of glucose concentrations tested on a single sensor chip. To demonstrate the longevity and stability of the fabricated device, the same sensor chip was used across the experiments, where the electrode was washed with distilled water after each measurement.

2.5. Adhesion of PSSs on CP electrodes

PSSs with a particle size of 10 μm and a pore size of 20 nm were purchased from Fuji Silysia Chemical Ltd., Japan. The specific surface area and pore size of the PSSs were obtained by deaeration at 150 °C for 3 h at 10^{-3} mmHg or less and the adsorption/desorption of nitrogen at −196 °C on a Belsorp-MAX II (Microtrac BEL Co. Ltd., Japan). The specific surface area was calculated by the Brunauer–Emmett–Teller (BET) method. The pore size was estimated by the Barrett–Joyner–Halenda (BJH) method applied to adsorption isotherms. The experiment was conducted in triplicates (N = 3), and the mean and standard deviation (SD) were determined. PSSs were sprinkled on the CP working electrode of the sensor chip immediately after the CH-N carbon ink was printed and when the ink has not yet dried and fully dried at 120 °C for 30 min for adhesion. Scanning electron microscopy (SEM) was used to observe the working electrode surface using an S-4800 (Hitachi, Ltd., Japan) system without a metal coating at an acceleration voltage of 1.5 kV.

3. Results and Discussion

3.1. Sensing of enzyme reactions using sensor chip

We first developed a sensor chip that can detect the enzymatic electrode reaction with a small amount of sample by screen-printing (Sect. 2.3, Fig. 1). The electrode part consists of a three-electrode system comprising a Pt or CP working electrode, a platinum counter electrode, and a Ag/AgCl reference electrode. The working electrode was 1 mm in diameter. Electrochemical analysis was performed by dropping 20 μL of sample (including enzyme, mediator, and electrolyte) onto the electrode [Fig. 1(e)].

The sensor chip was used to evaluate the electrochemical sensing performance of GDH in the glucose dehydrogenation reaction [see Eq. (1)]. Figure 2(a) shows potassium ferricyanide (PF)

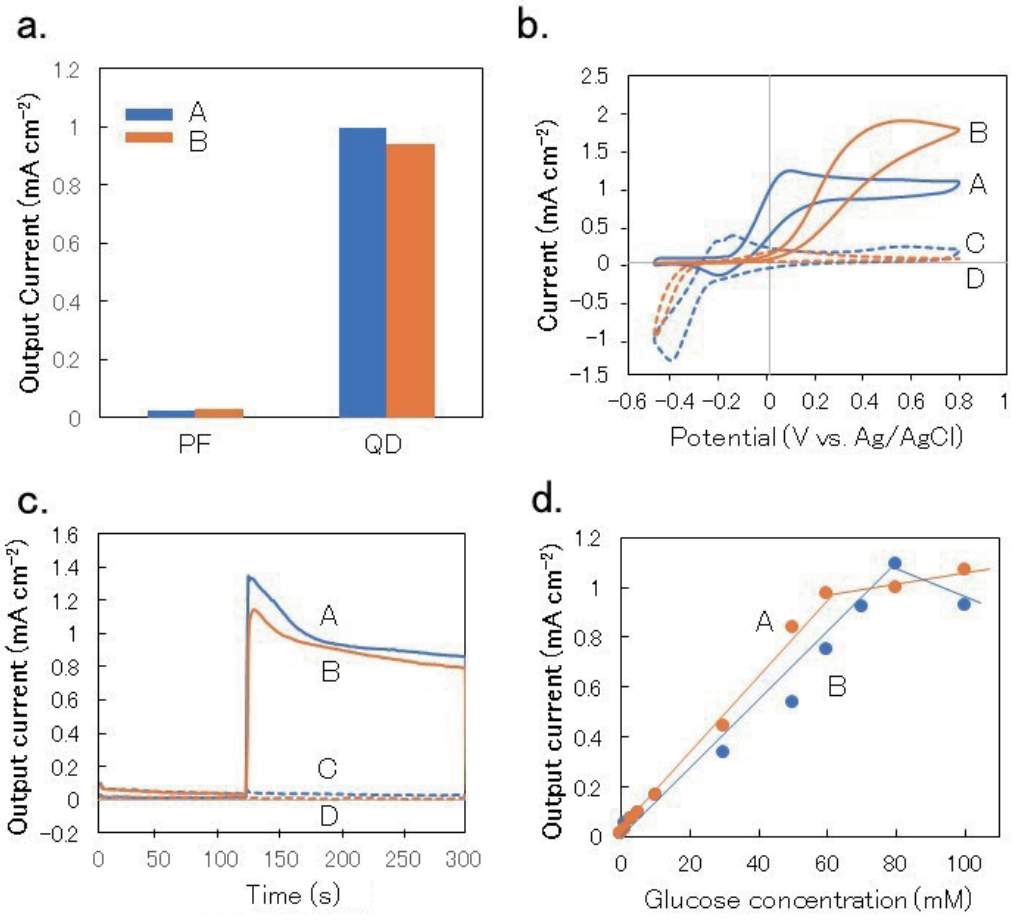

Fig. 2. (Color online) Evaluation of sensing GDH enzyme response with sensor chip. The blue bars, lines, and plots (A) indicate measurements with a Pt working electrode and the orange bars, lines, and plots (B) with a CP working electrode. (a) Comparison of output currents for different types of electron transfer mediator. (b) Comparison of cyclic voltammograms. (c) Comparison of amperometric responses. The dashed lines (blue C and orange D) show drops of solution without glucose, and the solid lines show drops of solution with glucose (blue A and orange B). (d) Calibration curve of output current at varying glucose concentration.

and QD as mediators of electron transfer since PF was considered the conventional mediator for electrochemical sensors.[5,6] No obvious output current could be detected when PF was used as a mediator. In contrast, significant output currents could be detected when QD was used as a mediator. QD was better than PF in this sensor system. Therefore, QD was used as a mediator in the following experiments.

In cyclic voltammograms [Fig. 2(b)], stable redox currents were detected at both the Pt and CP working electrodes. Here, especially in the CP working electrode, the QD reduction peak is significantly shifted to the minus side, and the oxidation peak is shifted to the plus side. However, its mechanism is unclear, and there is probably some interaction between carbon and QD. Similar output currents were obtained at both working electrodes in the amperometric reaction [Fig. 2(c)]. Figure 2(d) shows the calibration curve obtained by plotting the output current at varying glucose concentration. For the Pt working electrode, the plot values were nearly linear over the glucose concentration range of 1–80 mM; for the CP working electrode, they were nearly linear from 1 to 60 mM. The sensor's sensitivity is superior to the previously reported results of a glucose sensor using FAD-GDH and QD on a gold working electrode, which had an upper detection limit of 55.5 mM glucose.[33]

3.2. Enzyme immobilization on working electrode of sensor chip

Although we have used enzyme solutions in our evaluations with sensor chips so far, it was necessary to immobilize enzymes on the working electrode for practical applications to improve storage and repeated stabilities. We focused on PSSs, whose particle and pore sizes can be controlled, which was advantageous for enzyme immobilization because their well-defined pore structure and large surface area allowed for the uniform modification and encapsulation of enzymes. Figure 3(a) shows the N_2 adsorption/desorption isotherm of PSSs. Hysteresis was observed in the pressure range of 0.8–1.0, confirming the mesoporous structure of PSSs. Figure 3(b) shows the pore size distribution calculated by the BJH method. The PSS pore size averaged 22.5 nm with no significant variation (standard deviation of 0.64). Table 1 shows the pore diameter, pore volume, and specific surface area of PSSs.

However, the PSS itself was not suitable as an electrode material because it has no conductivity. If PSSs can be immobilized on an electrode and an optimal mediator can be used, the problem of electrical conductivity can be solved, and an enzyme-immobilized electrode can be produced. In fabricating the sensor, PSSs were sprinkled directly on the CP electrode immediately after the CP was printed. The layer was allowed to fully dry for the particles to adhere to the CP electrode. Figure 4 shows SEM images of the CP electrode without PSSs and the CP electrode with PSSs adhered (PSS-CP electrode). For the CP electrode without PSSs, the SEM image visually confirmed that the CP was uniformly printed [Fig. 4(a)]. When PSSs adhered to the CP electrode, the particles were self-arranged in a single layer on top of the CP, with the CP layer observable through the gaps between the particles [Fig. 4(b)].

Fifty microliters of GDH solution (28 U/μL) prepared at 10 times the concentration was dropped onto the PSS-CP electrode and left for 24 h at 4 °C to allow the enzymes to adsorb into and onto the PSSs. After the GDH solution was removed, the GDH-free mediator solution was

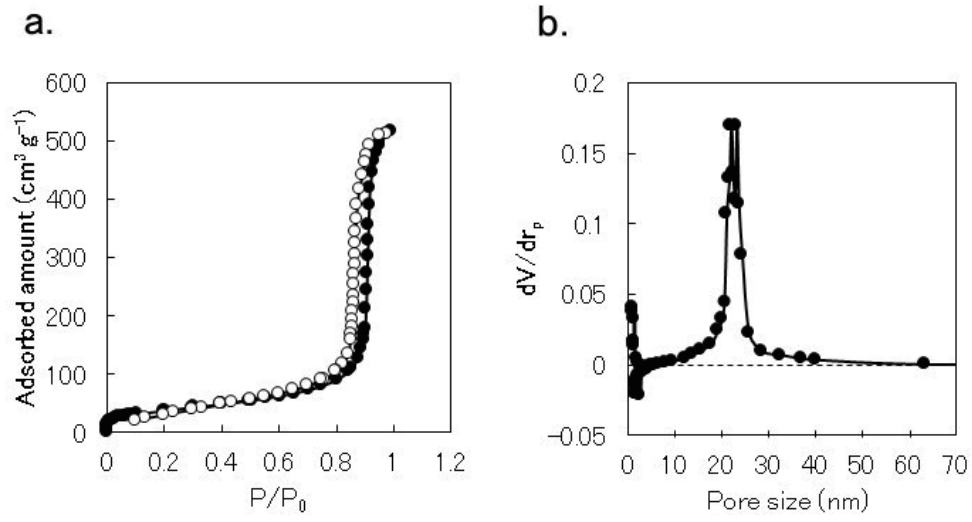

Fig. 3. (a) N_2 adsorption-desorption isotherms of PSSs measured at −196 °C. The black and white circle plots show the adsorption and desorption sides, respectively. (b) Pore size distribution plot of PSSs estimated by BJH methode.

Table 1
Porous properties of PSSs. The means and standard deviations (SD) of pore size, pore volume, and specific surface area obtained by three nitrogen gas adsorption methods are shown.

	Pore size (nm)	Pore volume ($cm^3\ g^{-1}$)	Specific surface area ($m^2\ g^{-1}$)
Mean	22.5	0.665	150
SD	0.64	0.003	11

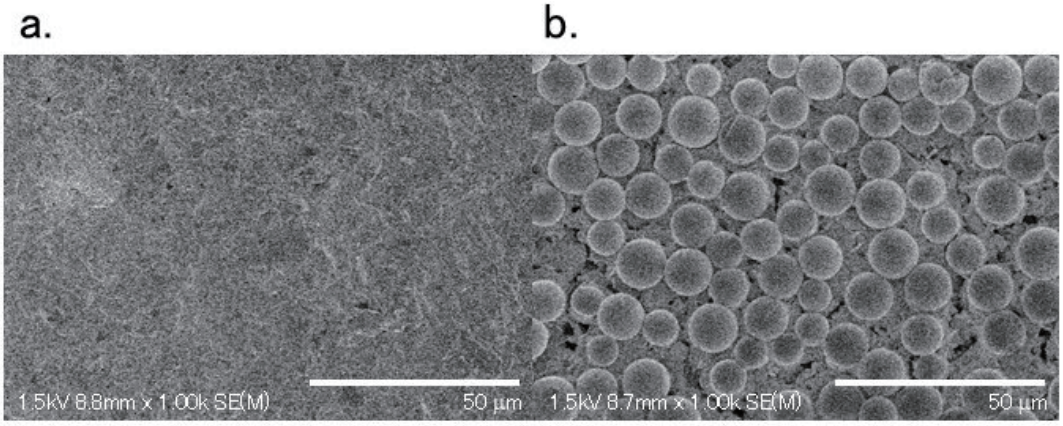

Fig. 4. (a) SEM image of CP working electrode without PSSs. (b) SEM image of CP electrode with PSSs adhered (PSS-CP electrode).

placed on the PSS-CP electrode. The target glucose solution was added onto the electrode, and the output current was examined by amperometric reaction [Fig. 5(a), orange B line]. The results were compared with the same setup on a CP electrode without PSSs (blue A line). Figure 5(a) shows that there was little change in reaction rate immediately after introducing glucose (comparable slope between Lines A and B). Figure 5(b) shows a calibration curve plotting the

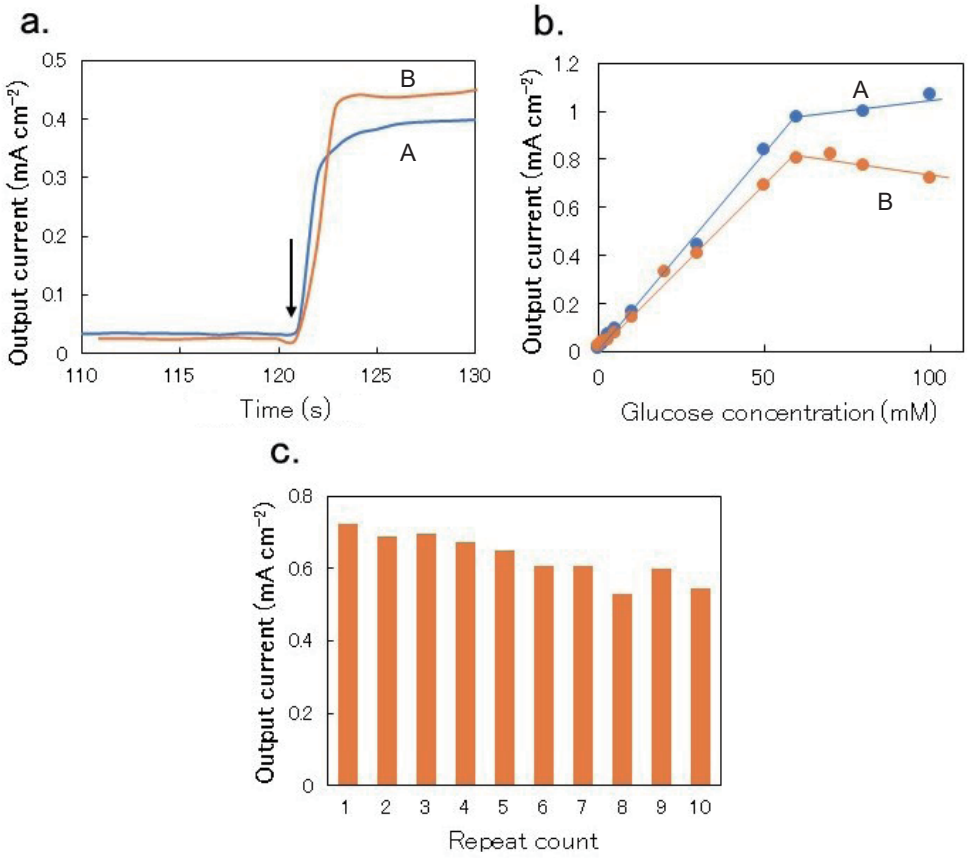

Fig. 5. (Color online) Evaluation of sensing of GDH enzyme reaction on GDH-immobilized PSS-CP working electrode. The blue lines (A) and plots (A) show measurements with GDH solution on the CP working electrode, and the orange lines (B), plots (B), and bars show measurements with GDH-free solution on the GDH-immobilized CP-PSS working electrode. (a) Comparison of amperometric responses. The glucose concentration was 30 mM, and the glucose solution was added at the arrow. (b) Calibration curve of output current at varying glucose concentration. (c) Stability of GDH-immobilized PSS-CP electrode for repeated measurements.

output current at varying glucose concentration at a GDH-immobilized CP-PSS electrode [orange (B) plot]. The plotted values for the CP-PSS electrode maintained a linear relationship from 1 to 60 mM, although the output current was moderately lower than that obtained with the GDH solution on a CP electrode [blue (A) plot]. This means that GDH was successfully immobilized on a CP electrode without loss of GDH activity. To evaluate the stability of PSSs on the CP electrode, we examined to what extent the output current was maintained when samples were repeatedly removed and dropped at the electrode [Fig. 5(c)]. A single sensor chip was used, and only the dropping solution was changed between measurements, with no washing process in between. No significant change in output current was observed after repeated measurements up to about 10 times. Thereafter, a gradual decrease in output current was observed, and after about 20 times, the output current decreased by half. This was likely due to the gradual detachment of PSSs from the CP electrode rather than enzyme inactivation, leaching or denaturation (Fig. S1). This is the first step to demonstrating a reusable device using PSSs on the CP electrode. More investigations are ongoing to improve the technique of retaining the PSSs on CP.

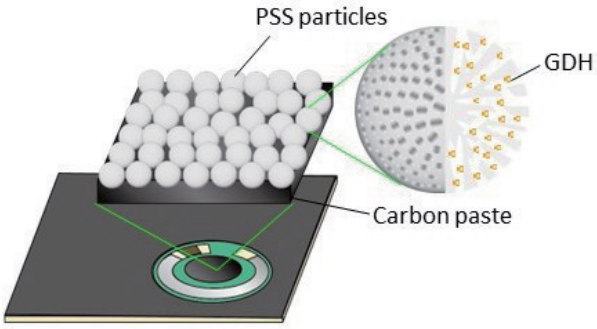

Fig. 6. (Color online) Schematic of GDH-immobilized PSS-CP electrode. A large amount of GDH is immobilized on the PPS owing to the pore structure of the PSS. The PPSs are arranged in a single layer on the CP electrode so that the electrons generated via the mediator in the GDH enzyme reaction are efficiently transferred to the CP electrode.

4. Conclusions

In this study, we presented an amperometric biosensing platform based on the immobilization of enzymes in PSSs that were screen-printed on a CP electrode. We demonstrated the sensor functionality using the GDH enzyme for glucose detection, but the sensor can be repurposed with other enzyme/substrate combinations. In conclusion, the methods described in this study demonstrate that PSS materials can be aligned by screen-printing on electrodes to provide a suitable support for the immobilization of enzymes (Fig. 6). This technique produces practical and easy-to-fabricate electrochemical biosensors that improve the tools' performance in terms of sensitivity, selectivity, and reusability. In addition, we are currently using a drop system, but in the future, we plan to form a flow path and incorporate it into repeat use.

References

1 M. Mayer and A. J. Baeumner: Chem. Rev. **119** (2019) 7996. https://doi.org/10.1021/acs.chemrev.8b00719
2 N. J. Forrow, G. S. Sanghera, S. J. Walters, and J. L. Watkin: Biosens. Bioelectron. **20** (2005) 1617. https://doi.org/10.1016/j.bios.2004.07.009
3 H. Jaegfeldt: J. Electroanal. Chem. **110** (1980) 295. https://doi.org/10.1016/S0022-0728(80)80381-0
4 G. F. Khan and W. Wernet: Anal. Chem. **69** (1997) 2682. https://doi.org/10.1021/ac961208z
5 T. Uemura, H. Yamazaki, T. Itoh, and S. Nishizawa: Anal. Sci. **38** (2022) 1189. https://doi.org/10.1007/s44211-022-00148-w
6 T. Uemura, S. Fujii, H. Yamazaki, T. Itoh, K. Masumoto, and S. Nishizawa: Sens. Mater. **34** (2022) 3173. https://doi.org/10.18494/SAM3914
7 H. Teymourian, A. Barfidokht, and J. Wang: Chem. Soc. Rev. **49** (2020) 7671. https://doi.org /10.1039/d0cs00304b
8 L. Xu, X. Zhang, Z. Wang, A. A. Haidry, Z. Yao, E. Haque, Y. Wang, G. Li, T. Daeneke, C. F. McConville, K. Kalantar-Zadeh, and A. Zavabeti: Nanoscale **13** (2021) 11017. https://doi.org/10.1039/D1NR02529E
9 B. Y. Zhang, A. Zavabeti, A. F. Chrimes, F. Haque, L. A. O'Dell, H. Khan, N. Syed, R. Datta, Y. Wang, and A. S. Chesman: Adv. Funct. Mater. **28** (2018) 1706006. https://doi.org/10.1002/adfm.201706006
10 S. D. Sprules, J. P. Hart, S. A. Wring, and R. Pittson: Anal. Chim. Acta **304** (1995) 17. https://doi.org/10.1016/0003-2670(94)00565-4
11 I. Shitanda, M. Mitsumoto, N. Loew, Y. Yoshihara, H. Watanabe, T. Mikawa, S. Tsujimura, M. Itagaki, and M. Motosuke: Electrochim. Acta **368** (2021) 137620. https://doi.org/10.1016/j.electacta.2020.137620
12 V. G. Gavalas and N. A. Chaniotakis: Anal. Chim. Acta **404** (2000) 67. https://doi.org/10.1016/S0003-

2670(99)00688-1
13 A. Parra, E. Casero, L. Vazquez, F. Pariente, and E. Lorenzo: Anal. Chim. Acta **555** (2006) 308. https://doi.org/10.1016/j.aca.2005.09.025
14 M. Gamero, F. Pariente, E. Lorenzo, and C. Alonso: Biosens. Bioelectron. **25** (2010) 2038. https://doi.org/10.1016/j.bios.2010.01.032
15 T. D. Gibson and J. R. Woodward: Biosensors and Chemical Sensors, P. G. Eldman and J. Wang, Eds. (American Chemical Society, Washington DC, 1992) p. 40.
16 F. Palmisano, G. E. De Benedetto, and C. G. Zambonin: Analyst **122** (1997) 365. https://doi.org/10.1039/A606849I
17 L. Doretti, D. Ferrara, P. Gattolin, and S. Lora: Talanta **44** (1997) 859. https://doi.org/10.1016/S0039-9140(96)02130-3
18 H. Li, Z. Guo, H. Wang, D. Cui, and X. Cai: Sens. Actuators, B **119** (2006) 419. https://doi.org/10.1016/j.snb.2005.12.041
19 B. Wang, B. Li, Q. Deng, and S. Dong: Anal. Chem. **70** (1998) 3170. https://doi.org/10.1021/ac980160h
20 B. Liu, R. Hu, and J. Deng: Anal. Chem. **69** (1997) 2343. https://doi.org/10.1021/ac960930u
21 J. Wang and N. Naser: Electroanalysis **6** (1994) 571. https://doi.org/10.1002/ELAN.1140060707
22 J. Qian, Y. Liu, H. Liu, T. Yu, and J. Deng: Anal. Biochem. **236** (1996) 208. https://doi.org/10.1006/abio.1996.0158
23 J. Fan, C. Yu, F. Gao, J. Lei, B. Tian, L. Wang, Q. Luo, B. Tu, W. Zhou, and D. Zhao: Angew. Chem. Int. Ed. **42** (2003) 3146. https://doi.org/10.1002/anie.200351027
24 J. L. Blin, C. Gérardin, C. Carteret, L. Rondehüser, C. Selve, and M. J. Stébé: Chem. Mater. **17** (2005) 1479. https://doi.org/10.1021/cm048033r
25 T. Shimomura, T. Itoh, T. Sumiya, F. Mizukami, and M. Ono: Sens. Actuators, B **135** (2008) 268. https://doi.org/10.1016/j.snb.2008.08.025
26 T. Itoh, Y. Shibuya, A. Yamaguchi, Y. Hoshikawa, O. Tanaike, T. Tsunoda, T. Hanaoka, S. Hamakawa, F. Mizukami, A. Hayashi, T. Kyotani, and G. D. Stucky: J. Mater. Chem. A **5** (2017) 20244. https://doi.org/10.1039/C7TA04859A
27 T. Itoh, T. Shimomura, A. Hayashi, A. Yamaguchi, N. Teramae, M. Ono, T. Tsunoda, F. Mizukami, G.D. Stucky, and T. Hanaoka: Analyst **139** (2014) 4654. https://doi.org/10.1039/C4AN00975D
28 T. Shimomura, T. Sumiya, M. Ono, T. Itoh, and T. Hanaoka: Anal. Bioanal. Chem. **405** (2013) 297. https://doi.org/10.1007/s00216-012-6494-5
29 T. Itoh, T. Shimomura, Y. Hasegawa, J. Mizuguchi, T. Hanaoka, A. Hayashi, A. Yamaguchi, N. Teramae, M. Ono, and F. Mizukami: J. Mater. Chem. **21** (2011) 251. https://doi.org/10.1039/C0JM01523G
30 T. Itoh, R. Ishii, T. Ebina, T. Hanaoka, Y. Fukushima, and F. Mizukami: Bioconjug. Chem. **17** (2006) 236. https://doi.org/10.1021/bc050238i
31 T. T. Chuong, T. Ogura, N. Hiyoshi, K. Takahashi, S. Lee, K. Hiraga, H. Iwase, A. Yamaguchi, K. Kamagata, E. Mano, S. Hamakawa, H. Nishihara, T. Kyotani, G. D. Stucky, and T. Itoh: ACS Appl. Mater. Interfaces **14** (2022) 26507. https://doi.org/10.1021/acsami.2c06318
32 S. Fujii, A. Yoshida, T. T. Chuong, Y. Minegishi, K. Pirabul, Z. Z. Pan, Y. Nishina, T. Kyotani, H. Nishihara, K. Masumoto, G. D. Stucky, and T. Itoh: ACS Appl. Engineer. Mater. **1** (2023), 1426. https://doi.org/10.1021/acsaenm.3c00103
33 J. Morshed, R. Nakagawa, M.M. Hossain, Y. Nishina, S. Tsujimura: Biosens. Bioelectron. **189** (2021) 113357. https://doi.org/10.1016/j.bios.2021.113357

Electronic supplementary information

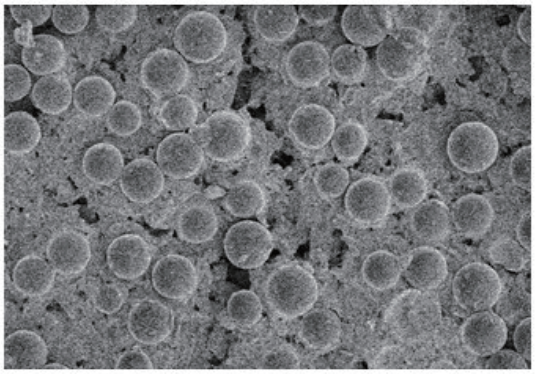

Fig. S1. SEM image of PSS-CP electrode surface after repeating the experiment 20 times. Figures 4(b) and S1 were taken at the same magnification.